CHALMERS
UNIVERSITY OF TECHNOLOGY

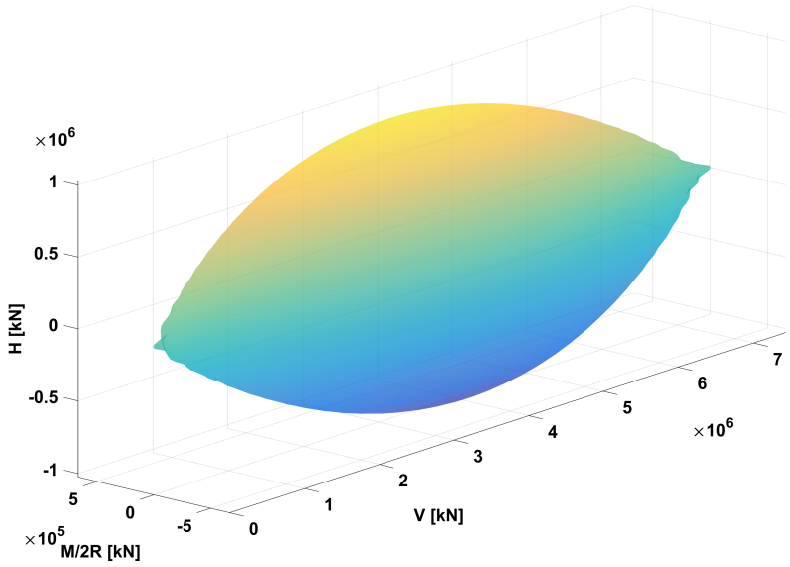

Geotechnical considerations of shallow wind turbine foundations on onshore locations in Sweden

An evaluation of the conventional method

Master's thesis in Infrastructure and Environmental Engineering

ELIN TUNANDER
ERIK JONSSON

Department of Architecture and Civil Engineering
CHALMERS UNIVERSITY OF TECHNOLOGY
Gothenburg, Sweden 2018

Master's thesis ACEX30-18-47

Geotechnical considerations of shallow wind turbine foundations on onshore locations in Sweden

An evaluation of the conventional method

ELIN TUNANDER
ERIK JONSSON

CHALMERS
UNIVERSITY OF TECHNOLOGY

Department of Architecture and Civil Engineering
Division of Geology and Geotechnics
Chalmers University of Technology
Gothenburg, Sweden 2018

Geotechnical considerations of shallow wind turbine foundations on onshore locations in Sweden
An evaluation of the conventional method
ELIN TUNANDER
ERIK JONSSON

Supervisor: Jelke Dijkstra, Department of Architecture and Civil Engineering
Industry Supervisor: Alexandre Mathern, NCC and PhD at Structural Engineering
Examiner: Jelke Dijkstra, Department of Architecture and Civil Engineering

Master's Thesis ACEX30-18-47
Department of Architecture and Civil Engineering
Division of Geology and Geotechnics
Chalmers University of Technology
SE-412 96 Gothenburg
Telephone +46 31 772 1000

Cover: Three dimensional failure envelope.

Typeset in LaTeX
Gothenburg, Sweden 2018

Geotechnical considerations of shallow wind turbine foundations on onshore locations in Sweden
En evaluation of the conventional method
ELIN TUNANDER
ERIK JONSSON
Department of Architecture and Civil Engineering
Chalmers University of Technology

Abstract

Expansion of onshore wind turbines are increasing due to its green energy and low costs compared to offshore. The turbines are getting larger to produce more energy which means the foundations are increasing to carry the larger loads. The loads are a combination of vertical, horizontal and moment of force loading. These loads can be either; static, quasi-static or dynamic. For the design methods of this study the loads are considered static. A large share of the ecological cost of a wind turbine comes from the material used in the foundation. The aim of this study was to consider the geotechnical aspects of wind turbine foundations for an onshore location in Sweden, with a shallow foundation subjected to combined loading.

To evaluate the safety of a foundation two considerations are usually made; ultimate limit state (ULS) and serviceability limit state (SLS), where the first is more concerned with stability and the latter with loss of function due to excessive deformations. The focus of this study has been on ULS. The stability of a foundation is conventionally done with empirically developed formulas. These formulas has many weaknesses, so numerical methods has been developed to calculate more accurate results. The two numerical methods used in this project was LimitState:GEO (LSG) and Optum G3.

A theory to approximate the ULS is the yield surface approach; a three-dimensional failure envelope for shallow foundations. By calculating the ULS with three loading types, a cigar shaped surface will take form. A case study was made to create such a yield surface with the 3D geotechnical finite element software Optum G3. 3D is necessary because it can calculate the three loading types and it incorporates the stress distribution below the footing in a way that is not possible in 2D. The case study has been made with a windturbine located on a dense coarse grained till material. Before the calculations for the yield surface was made, Optum and the 3D model was tested and verified with LSG and theoretical calculations.

The resulting yield surface was in good agreement with the literature study. An equation was formulated which proved to be valid for different sizes of the foundation. It was concluded that the foundation in this study is oversized from a stability perspective and could be designed to be smaller.

Keywords: on-shore, windturbine, shallow foundation, yield surface, combined loading, limit state analysis, Optum, LimitState:GEO

Acknowledgements

This thesis has been a collaboration between NCC in Gothenburg and the Division of Geology and Geotechnics.

We want to thank our examiner and supervisor Dr. Jelke Dijkstra for his guidance, support, encouragement and advises during this thesis. We would also send our gratitude to our supervisor Alexandre Mathern, Prof. Minna Karstunen and Lars Hall at NCC for their feedback and support. A special thanks to Tomas Törnkvist that provided us with data used in our case study.

Erik Jonsson, Elin Tunander, Gothenburg, June 2018

Contents

List of Figures

List of Tables

1
Introduction

1.1 Background

1.1.1 Expansion of wind turbines

The expansion of wind turbines has increased significantly both in Sweden and internationally in the last years (Energimyndigheten, 2014). In 2015, wind turbines contributed to approximately 10 percent of the total produced electricity in Sweden, compared to 2006 when it was half a percent. Sweden has a goal that by 2040 the production of electricity will be completely by renewable sources and wind energy is a source that can contribute to reach this goal. By 2020 the yearly production of electricity from wind turbines should be 30 TWh and this can be compared to today's production of 17.5 TWh. To achieve this goal it is necessary to build several hundreds of new wind turbines annually. When building a new wind turbine it is important to consider several aspects such as effects on humans (e.g. noise, visual impact and safety), animals and the environment, in this project, however, only geotechnical aspects will be considered (Boverket, 2009).

Wind turbines can either be situated onshore or offshore (Jacobsson et al., 2014). The diffusion of wind turbines in Sweden has taken place mainly onshore, even though one might argue that the expansion for offshore wind farms is preferable considering the large sea areas surrounding Sweden. At the moment onshore is still a popular alternative due to the low costs, which can be seen in the northern parts of Sweden where Europe's largest onshore wind farm is planned to be operational by 2019 (Froese, 2017).

Together with the expansion of wind turbines, they have become larger and more efficient. Increased height of wind turbine towers gives a higher energy production due to higher wind velocities. At the same time, the size of the foundation increases due to larger loads acting on the foundation (Shrestha and Ravichandran, 2015).

1.1.2 Foundations for wind turbines

The foundation of a wind turbine is the interface between the superstructure and the ground which transfers loads acting on the wind turbine tower down to the underlying soil in a process called soil-structure interaction (Warren-Codrington, 2013). Wind loads on the structure and rotating components in the turbine as well as the

self weight gives a combined load on the foundation that consists of vertical, horizontal and moment forces. For wind turbines, the vertical forces are minor and it is the overturning moment at the base of the tower that is the governing factor when designing the foundation (Burton et al., 2011). The traditional design method are not able to accurately predict the bearing capacity of these foundations subjected to combined loading.

There are different types of foundations for wind turbines depending on the underlying soil, e.g. on bedrock it is common that the foundation is shallow and fixed to the rock with bolts (Mohamed, 2016). Shallow gravity foundation can also be used on competent soils, i.e. soils that can fulfill stability and settlement criteria without further improvements. In weak soils where the soil cannot carry the load, shallow foundation will not work, and instead a deep foundation, which are more expensive and have a long construction time, should be considered. Therefore, if possible a shallow gravity foundation is a more viable option from an economical perspective compared to piling.

Even though they are less expensive, a shallow gravity foundation also constitutes a large share of the total cost of the wind turbine structure. With this in mind, it is of interest to investigate if the foundation design could be optimized in order to minimize the cost and material usage.

1.2 Aim and objectives

The aim of this study is to consider the geotechnical aspects of wind turbine foundations on onshore locations in Sweden, with shallow foundations subjected to combined loading (vertical, horizontal and moment of force loading). The following objectives are formulated:

- To create a failure envelope for combined loading using three dimensional finite element analyses.
- To evaluate the conventional design method for shallow foundations against an advanced numerical limit state method.
- To discuss the implications of current evaluation methods, considering a typical Swedish scenario.

2

Theory

2.1 Foundation loads

The foundation of the wind turbine is subjected to both static and variable loads which can be quasi-static or dynamic. In the quasi-static case the inertial forces are negligible, whilst for the dynamic case the inertial forces cannot be neglected (Wichtmann, 2005). The shallow foundation considered in this research, is subjected to two different forces and one overturning moment. Forces in vertical direction is mainly self weight, in horizontal direction it is generated by the wind and the overturning moment occur due to wind loads acting high above foundation level. The overturning moment is the most significant load (Byrne, 2011). See Figure 2.1.

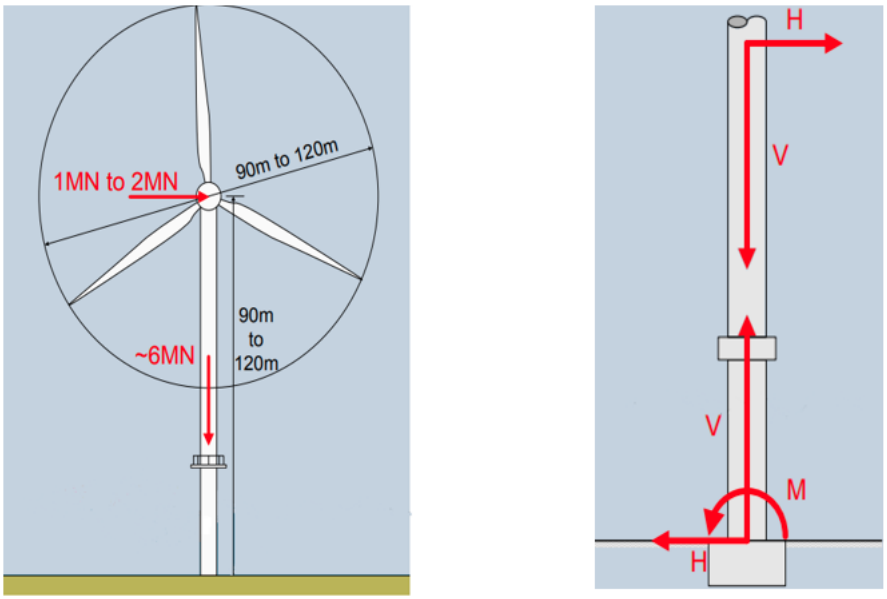

Figure 2.1: Loads on the foundation where self weight goes in vertical direction (V), wind load mainly in horizontal direction (H), and overturning moment (M) because of wind loads acting on the hub high above the ground level (Byrne, 2011).

Self weight of the structure (dead load) is static, rotation of the blades has two frequencies, one from rotation and one from the shadowing of the blades which can be considered quasi-static (Bhattacharya, 2017). These loads are cyclic in nature.

In the design methods considered below, the loads are considered static where any quasi-static or dynamic effects are not explicitly taken into account.

2.2 Limit state analysis

The bearing capacity of a soil is the maximum average contact pressure allowed between soil and structure without producing shear failure in the ground (Knappett, 2012). For a satisfactory design of a foundation two performance requirements need to be met:

1. such that its capacity or resistance is sufficient to support the loads (actions) applied (i.e so that it does not collapse).
2. to avoid excessive deformation under these applied loads which might damage the supported structure or lead to a loss of function.

These criteria are commonly factored into two states; ultimate limit state (ULS) which is collapse or instability of the structure as a whole, or the failure of one of its components. The other is serviceability limit state (SLS) which involves excessive deformation, leading to loss of function.

2.2.1 Ultimate limit state

From a geotechnical point of view, ultimate limit state is referring to the stability of the structure (Knappett, 2012). To not produce failure in regards to the ultimate limit state, the sum of all applied loads of the foundation should at least be equal or less than the available resistance. Structural elements of the foundation should be proportioned so that they can resist the most critical load combinations.

The first methods developed to calculate the ultimate bearing capacity are limit equilibrium methods which calculates the stability for an arbitrary failure mechanism (Sloan, 2013). In the methods the equilibrium and compatibility is not satisfied throughout the whole domain. For a more rigorous solution of the stresses and the strains occurring in the ground it is necessary to have three different types of equations; equilibrium conditions, constitutive relations, and compatibility equations (Verruijt and Van Baars, 2007). Except for very limited cases these three equations are extremely difficult to achieve. A way to solve this situation is to use limit analysis which is based on plasticity theory. The limit analysis uses two different theorems where one is based on an equilibrium system or a statically admissible stress field and the other is based on a mechanism or a kinematically admissible field of displacement. The first theorem will give a lower bound solution and the latter an upper bound solution.

A statically admissible stress field is one that satisfies the following conditions according to Verruijt and Van Baars (2007):

- equilibrium in each point
- boundary conditions for the stresses
- yield condition is not exceeded in any point

A kinematically admissible field of displacement is one that satisfies the following conditions according to Verruijt and Van Baars (2007):

- displacement field is compatible
- boundary conditions for the displacements
- stresses fulfill the yield condition wherever deformations take place

It can be shown that the true failure load is larger than the load that corresponds to the lower bound and is smaller than the load that corresponds to the upper bound. The exact solution of the failure load is obtained when these two solutions give the same results which can be referred as a closed form solution.

2.2.1.1 Development of bearing capacity equation

Prandtl (1920) was the first to find an exact solution for the ultimate bearing capacity of a foundation and has the closed form $(2+\pi)c$ (Verruijt and Van Baars, 2007). The Prandtl solution is only valid for a cohesive, weightless homogeneous soil which is far from practical real situations. Unfortunately, there are no closed-form solution for frictional soils or more complex layering or load combinations. The exact solution of Prandtl have been developed over the years by several investigators to make it more usable in practice. Terzaghi (1944) developed a formula for general shear failure for a shallow strip foundation, which also take into account the self weight of the soil. Empirical correction factors have later been derived such as shape factor s that take into account if the foundation is not infinitely long (Knappett, 2012). When the failure mechanism below the foundation is three dimensional, such as a circular foundation, the accuracy of the shape factors is inadequate. Furthermore, to incorporate both vertical and horizontal actions, the formula has been extended with an additional inclination factor i. If the inclined load also works with an eccentricity e from the centre line, the moment of force will also be included in the analysis. This results in a reduced uniformly effective width of the foundation, b_{eff}. Within the effective area the ground pressure is assumed to be uniformed distributed. The complete drained bearing capacity formula with all factors can be calculated according to Equation 2.1 (DNV, 2002)

$$q = \frac{1}{2}\gamma^{'} b_{eff} N_\gamma s_\gamma i_\gamma + p_0^{'} N_q s_q i_q + c N_c s_c i_c \tag{2.1}$$

N_γ, N_q and N_c = bearing capacity factors all depending on the friction angle, $\phi^{'}$[-]
i_γ, i_q and i_c = inclination factors [-]
s_γ, s_q and s_c = shape factors [-]
c = cohesion [kPa]
$p_0^{'}$ =effective overburden pressure at the level of the foundation-soil interface [kPa]
γ' = effective unit weight of soil [kN/m^3]
b_{eff}=effective width of foundation [m]

In Eurocode partial factors are used in order to be on the safe side when designing constructions. Design values are used by decreasing soil strength parameters and increasing acting loads. Explanation for the parameters in Equation 2.1 can be found in Appendix B where the design values are included. Several investigators have derived formulas for the bearing capacity factors N. They are dependent on the friction angle and can be calculated as follows:

$$N_q = e^{\pi tan\phi}\frac{1+sin\phi}{1-sin\phi} \quad N_c = (N_q - 1)cot\phi \quad N_\gamma = \frac{3}{2}(N_q - 1)tan\phi \tag{2.2}$$

If the foundation is embedded at a depth d, the soil above the foundation level will act as a surcharge, i.e. uniform pressure, and then $p_0^{'} = d\gamma$ (Knappett, 2012). It is worth noting that the shear strength of the soil above the foundation level is not included in the bearing capacity formula.

Depending on where the water table is situated, different unit weight in Equation 2.1 for an effective stress analysis should be used. If the water table is well below the foundation, total unit weight γ should be used in the first term and second term. With the water table at foundation level effective unit weight, γ' must be considered in the first term and total in the second. If the water table is at ground level effective unit weight γ' should be used in both terms. If the water table is between foundation level and ground level Equation 2.3 should be used to calculate the surcharge by the soil and if the water table is situated within a depth less than the effective width of the foundation, Equation 2.4 should be used for an equivalent weight of the soil in the first term (IEG, 2010).

$$p_0^{'} = \gamma d_1 + \gamma' d_2 \tag{2.3}$$

where d_1 is the distance between ground level and water table level, and d_2 is the distance between lowest point of the foundation and water table level.

$$\gamma_{eq} = \gamma\frac{d_2}{b_{eff}} + \gamma^{'}\frac{b_{eff} - d_2}{b_{eff}} \tag{2.4}$$

2.2.1.2 Development of numerical methods

The bearing capacity formula described above has severe limitations in coarse grained material, complex geometrical shapes, layered soil and combined loading to name a few. To overcome these weaknesses several numerical methods for solving the resulting system of equations from plasticity theory have been developed in the last decades. The accuracy of the resulting solutions depends on the numerical implementation. In addition many of the numerical techniques only approximate one of the two bounds.

The two numerical methods used in this project; LimitState:GEO (LSG) and Optum G3 are examples of this. LSG, which is a 2D method, calculates the upper bound. Optum on the other hand, which is a 3D method, estimates both the upper and the

lower bound solution, as well as a mixed formulation which suggest a compromise where both the stress and displacements are the primary variables.

This project considers a wind turbine foundation on coarse grained soil. Since wind turbines are exposed to forces coming from multiple directions, the problem is better solved with a method that considers three than two dimensions.

2.2.2 Serviceability limit state

Serviceability limit state is associated with three performance functions, affecting the structure's operation (Ahmed and Soubra, 2014). These functions are defined as the limit for when tolerable horizontal and vertical displacements as well as rotation of the foundation are exceeded. Under working loads, the pressure from a shallow foundation is usually much less than its capacity in regards to stability.

For a wind turbine foundation the definition of serviceability limit state is not straight-forward. In addition to the settlements due to the self-weight of the structure, significant deformations can be expected under the operational loads discussed in Section 2.1. Settlements of the structure may not only have a great negative impact on the operation of the wind turbine, but also on the stability. If one edge of the foundation settles more than the other, this will result in a reduction of the effective area in contact with the subsoil (Ntambakwa et al., 2016).

Settlements are closely related to the stiffness of the soil. In coarse grained material, which is considered in the case study, the static load immediately leads to deformations, which results from a combination of volumetric and shear strains. Depending on the characteristic time for quasi-static loading, T_l and the characteristic time for consolidation, T_c not all pore pressure will be dissipated during the load cycle ($T_l > T_c$), and the excess pore pressure will accumulate. This will affect both the stability and the stiffness below the foundation. In this case the shear strains will dominate. Under the operational loads of the wind turbine, the stiffness of the subsoil influences the magnitude of the dynamic loads in the structure. This so called soil-structure-interaction problem requires considerations of the structure, the foundation and the subsoil in the calculation.

Because of the discrete nature of soils the stiffness response is non-linear and depending on the effective stress level and the loading amplitude. At very small values of shear strains, the shear modulus, G, is represented by a maximum shear modulus G_{max}, which originates at a particle to particle contact level. This is referred to as the small strain shear modulus, G_{max} or G_0. G_{max} is independent of shear strain, the number of small strain loading cycles and the initial density, but is dependent on effective stress (Wichtmann, 2005). The shear degradation curve shown in Figure 2.2 is non-linear, and describes the relationship between the ratio G/G_{max} versus the shear strain amplitude. The curve is normalized with the shear modulus at small strains G_{max}, which makes the curve universal for all effective stress levels.

Below a certain strain amplitude, the G is approximated to be equal to G_{max}. For larger strain amplitudes, the G is a function of the shear strain, and decreases with increasing shear strains and plastic deformation occurs.

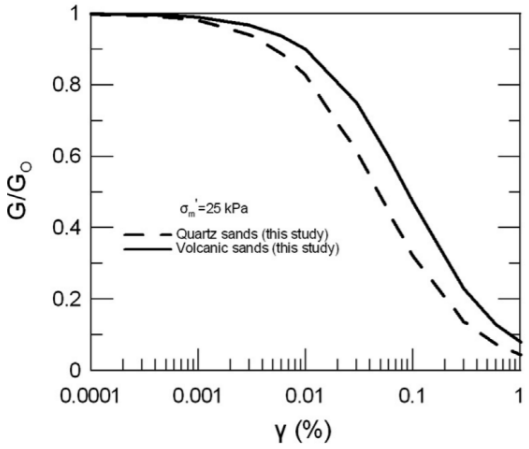

Figure 2.2: Example of a non-linear G/G_{max}-logγ curve, for quartz and volcanic sands (Senetakis et al., 2013).

2.3 Yield surface approach

The yield surface approach for soil is a method first suggested by Butterfield and Gottardi (1994) which is a complete three-dimensional failure envelope for shallow foundations. Their hypothesis was that there exists a relation between vertical, horizontal and moment of force loading in regards to when failure of the soil occurs. They tested different combinations of these three loading types to find when the soil failed which was then plotted in a three dimensional space. Each axis corresponded to one of the mentioned loading types, with the moment of force loading divided by the diameter of the foundation. With many point data of this sort a surface took shape, similar to a cigar, containing all the combinations that will cause failure of the soil. Butterfield and Gottardi (1994) defined this three-dimensional failure envelope with the general formula in Equation 2.5, with C being defined by Equation 2.6.

$$(\frac{H}{t_h})^2 + (\frac{M}{Bt_m})^2 - \frac{2CMH}{Bt_h t_m} = [\frac{V}{V_{max}}(V_{max} - V)]^2 \tag{2.5}$$

$$C = tan(2\rho)(t_h - t_m)(t_h + t_m)/(2t_h t_m) \tag{2.6}$$

H=horizontal loading
M=moment of force loading
V=vertical loading
V_{max}=central vertical load capacity of the footing
t_h=initial angle of yield surface in the V-H plane
t_m=initial angle of yield surface in the V-M/B plane

B=diameter of footing
ρ=tilt angle of the yield surface in M/B-H plane away from the H axis

The advantage with representing the stability of the earth in this way is that it represents a more realistic and comprehensive response than more general stability calculations, like the bearing capacity formula described in chapter 2.2.1.1 as well as for sliding and overturning. Byrne (2000) described the definition of a yield surface in (V:M/B:H) space for a strip footing of width B, or in (V:$M/2R$:H) space for a footing of radius R as "if the load state of the foundation is such that it touches or exists outside the yield surface then plastic displacements occur, otherwise the response of the foundation is elastic".

The major advantage with this method is that the stability of the foundation can be easily assessed. By simply plotting a load case in the same figure as the yield surface to find it lies within the boundaries, the foundation is deemed as safe and the response as elastic. However, if it falls outside the yield surface the foundation response will be plastic.

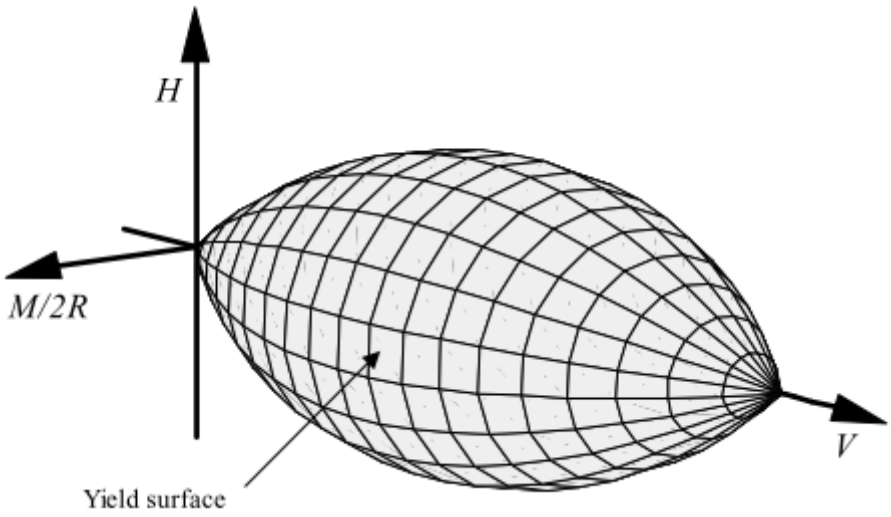

Figure 2.3: Example of yield surface (Byrne, 2000).

There are two fundamental applications of this theory for the design of wind turbine foundations:

1. Wind turbines with shallow foundations are particularly vulnerable to horizontal and moment loading with $H_{max} \approx V_{max}/8$ or $M_{max}/2R \approx V_{max}/11$ being enough to cause failure (Butterfield and Gottardi, 1994). This is why foundations exposed to high lateral loads are often piled or founded at sufficient depth.

2. It is problematic to achieve a high factor of safety if a foundation is exposed to an increase in H or M while at the same time having a low V.

The size of the yield surface is strongly connected to the size of V_{max} which is the estimated vertical component capacity of the footing, without a horizontal component or bending moment. H_{max} and $M_{max}/2R$ are both located at $V{=}V_{max}/2$.

2.4 Numerical solutions for ultimate limit state

2.4.1 Optum G3

Optum G3 is a geotechnical finite element program that can calculate the ULS of a three dimensional case with applied vertical, horizontal and moment of force loading. By establishing the relative size of these three loading types, it is possible to calculate an adequacy factor that corresponds to the number of magnitudes until failure of the soil occurs. The program was released in 2018 and is a further development of its two dimensional counter part Optum G2.

Optum G3 has the ability to perform limit analyses according to rigorous upper and lower bound principles on collapse loads, as well as a mix of the two (K Krabbenhoft, 2016b). Rather than facilitating the computation of rigorous bounds this principle makes various 'compromise' solutions. This solution cannot be rigorously bounded but tends to be closer to the exact solution than either of the rigorous upper and lower solutions. The mixed solution suggests that a compromise is made where both the stress and displacements are the primary variables.

In Optum, the Mohr-Coulomb material is a solid material that can be applied to volumetric objects. It is a material that has a yield function defined by two parameters, cohesion c' and friction angle ϕ', and assumes linear elasticity. The flow rule is generally nonassociated and defined by a dilation angle and, optionally, a dilation cut-off (K Krabbenhoft, 2016a).

2.4.2 LimitState:GEO

LimitState:GEO (LSG) is a numerical program that calculates the ultimate limit state to solve geotechnical problems. It is a 2D program using the Discontinuity Layout Optimization (DLO) procedure (LimitState, 2016). DLO is a limit analysis method which gives the upper bound solution based on formal plasticity theory. How the procedure works can be seen in Figure 2.4. After the problem has been identified the soil is discretized with nodes (Gilbert et al., 2010). The nodes are thereafter connected with potential lines of discontinuity, i.e. slip lines. By mathematical optimization the critical layout of lines of discontinuity at failure can be identified by finding the subset of potential discontinuities that will have the lowest energy dissipation, i.e. find the mechanism that will cause failure with the least load.

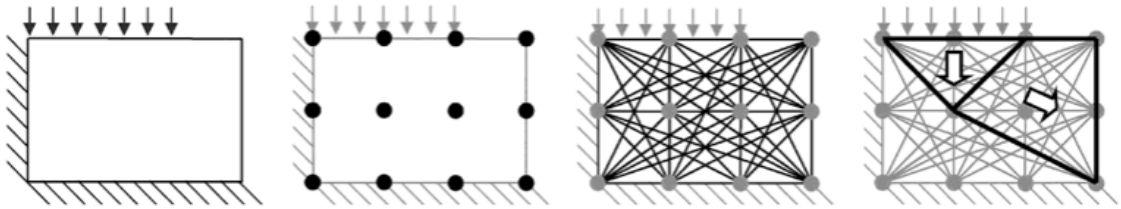

Figure 2.4: Procedure of Discontinuity Layout Optimization (Gilbert et al., 2010).

To define stress-strain behaviour of the soil, different material models are available in LSG, that is Mohr-Coulomb, tension and/or compression cut off, rigid or engineering element (LimitState, 2016). A Mohr-Coulomb material is a linear relationship between normal stress and shear strain. The linear relationship is defined in LSG for drained analysis by parameters ϕ' and c' and for undrained analysis c_u. By combining material models the yield behaviour of the soil can be more complex and non-linear.
In order to obtain the ULS it is necessary to drive the system to collapse (LimitState, 2016). This can be done either by increasing the specified loads or reducing the soil strength. The solution is represented as an adequacy factor. The adequacy factor is the factor that the existing loads must be increased, or material strengths decreased to drive the system to collapse.

2.4.2.1 Effects of nodal density and domain size

If there are more nodes used in the analysis more discontinuity lines are generated and will give a more accurate solution (LimitState, 2016). What is not explicitly clear in the manual, however, is that to get a solution as close as possible to the "exact" solution, the nodal resolution should be progressively refined. LimitState:GEO has predefined amount of nodes of 250, 500, 1000 and 2000 as nodal density. When choosing a nodal density for a model, a specific distance between each node will be made. If the same model will be enlarged, the distance between the nodes will increase and will in turn give a less accurate result. To keep the same nodal density and hence the same spacing between nodes for different model sizes, the setting *custom* can be used where the amount of nodes can be altered. In addition, to use a sufficiently fine nodal density it is important to choose a suitable domain that is sufficiently large to not influence the solution. It is likely that the boundaries do not influence the solution if the failure lines do not intersect or touch any of the boundaries. A study of nodal density and model size of the solution can be seen in Figure 2.5 and 2.6. The model size is not very important but it has to be sufficiently large. Increased nodal density improves the accuracy of the solution at the cost of computational time. Furthermore, as will be seen in the following chapter, calculated theoretical value from Equation 2.1 is lower than results from LSG which was expected when LSG gives the upper bound solution.

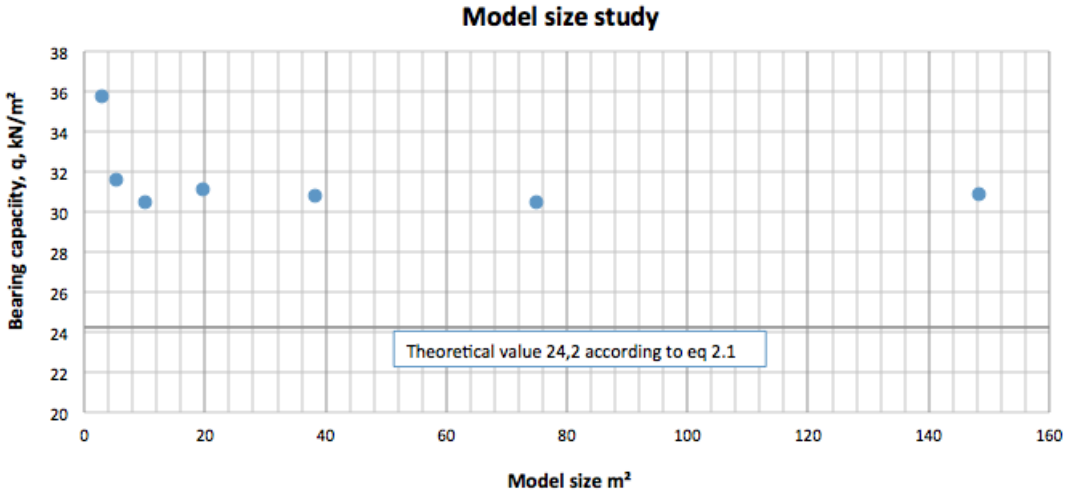

Figure 2.5: Results from study with LimitState:GEO with different model sizes compared to theoretical value taken from equation 2.1 (surface footing subjected to a vertical load where $q = \frac{1}{2}N_\gamma$ with a friction angle of 37 °)

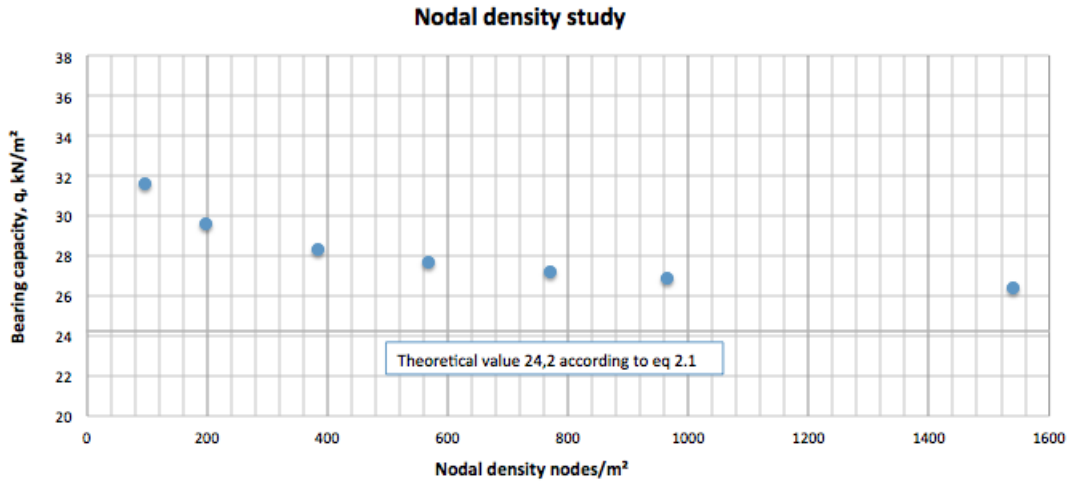

Figure 2.6: Results from study with LimitState:GEO with different nodal density compared to theoretical value taken from equation 2.1 (surface footing subjected to a vertical load where $q = \frac{1}{2}N_\gamma$ with a friction angle of 37 °)

3
Methodology

3.1 Case study: 3D model in Optum G3

One of the goals with this study was to create a yield surface for a real case in Sweden. There are some important aspects for using a 3D program when modelling the wind turbine foundation. First, it is possible to combine the three loading types; vertical, horizontal and moment of force. It is also possible to model the horizontal and moment of force loading in the opposite directions. To an extent this may also be possible in 2D, however, in 3D it also incorporates the stress distribution below the footing in a way that would not be possible in 2D. A footing that could be of different shapes and have an eccentric applied loading. This is why Optum G3 has been used to calculate the failure loads.

The case study is based on a real project for a typical soil located in the northern parts of Sweden where many wind farms are located and planned to be constructed in the future (Froese, 2017). All the following properties of the location, foundation and design load cases are based on an existing project.

3.1.1 Geotechnical properties of the wind turbine location

The location of the wind turbine has an underlying soil that consists of a dense coarse grained till material. 75 % of Sweden is covered by till which makes it the most common soil type in Sweden (SGI, 2018). The water table is situated 1.23 meters below surface level. The till consists mainly of sand with some gravel and silt mixed in, and has the following properties:

$\gamma_{dry} = 20$ kN/m^3
$\gamma_{saturated} = 22$ kN/m^3
$E_k = 35$ MPa
$\phi = 37$ °
$c = 0$ kPa
Dynamic probing was used as ground investigation method to determine friction angle and elasticity modulus. The density of the soil is taken from empirical guideline values. In Optum, the soil was assumed to be drained and consist of a Mohr-Coloumb material. Since Optum does not include a feature for drained conditions, $\gamma_{saturated}$ was reduced by 10 kN/m^3 to account for the pore water pressure.

Figure 3.1: Profile of soil depth.

3.1.2 Geometry of foundation and load application

The foundation footing that is used in the calculations is round and have a diameter of 23.8 meters. A short pedestal that connects to the wind turbine is included on top as well as a truncated cone shaped slab on the bottom. The material is assumed to be rigid and have a self weight of 25 kN/m^3 which is the weight for concrete (Asp, 2016). The exact geometry can be seen in figure 3.2.

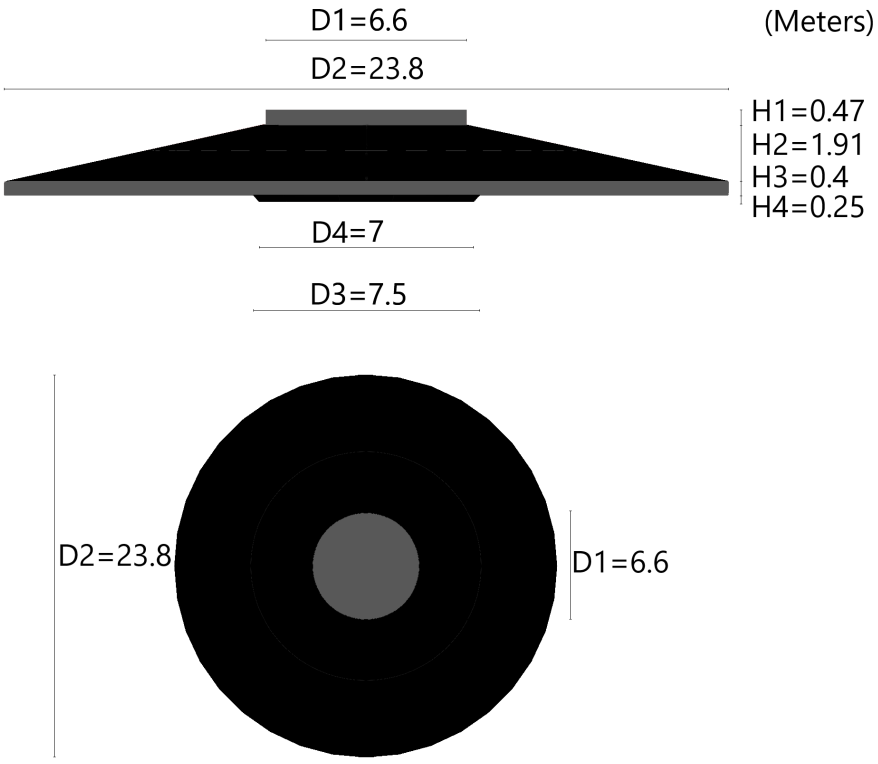

Figure 3.2: Geometry of wind turbine foundation.

The vertical and horizontal forces are evenly spread out on top of the foundation's pedestal. The moment of force loading is applied along a line perpendicular to the horizontal load on top of the foundation. The forces can be seen in Figure 3.3.

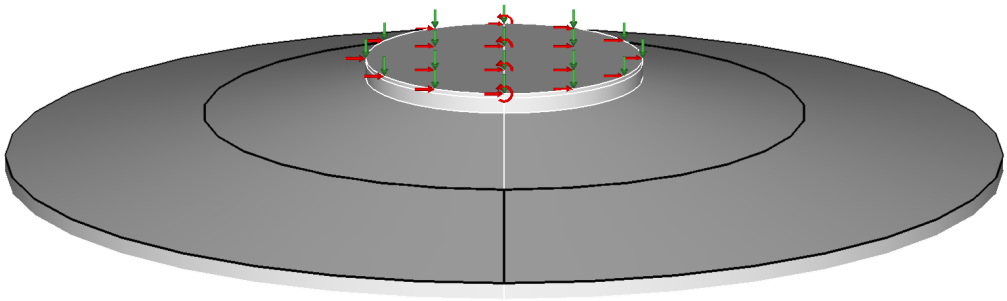

Figure 3.3: Applied acting forces on the foundation.

3.2 Verification of 3D model

Before the foundation model in Optum can be used, validation of size of the soil domain has to be made to reassure that the borders are not interfering. Furthermore, the calculated results has to be verified with other calculation methods. This was done by starting with creating simplified models in Optum and LimitState:GEO (LSG), that could be compared to each other and theoretical calculations.

3.2.1 Sensitivity analysis of soil domain size

The Optum model that will be used has to be tested in order to get realistic results. Four different model geometries were created and used to simulate the failure load with the same applied forces. The size of the four models' soil domains were 130×130×75 meters, 150×150×75 meters, 200×200×100 meters and 250×250×150 meters. The calculation was made with adaptive iteration and an increasing number of elements. This means that first a calculation with fewer elements was made, followed by another calculation with more elements. The finer mesh is based on the result from the previous step in order to avoid partitioning parts of the mesh unaffected by the load and in that way optimize the mesh.

Table 3.1: Total stress under the foundation required to cause failure in the Optum models due to vertical loading (V_{max}) [m].

No of elements	130×130×75 [kPa]	150×150×75 [kPa]	200×200×100 [kPa]	250×250×150 [kPa]
≈ 2100	3894	5638	5233	3748
≈ 5000	12927	11304	13066	12696
≈ 15000	16295	16426	16295	16165
≈ 24000	16518	16611	16565	16565
≈ 32000	16680	16711	16634	16641
≈ 41000	16718	16695	16672	16726

Table 3.2: Total stress under the foundation required to cause failure in the Optum models due to combined vertical and horizontal loading (relative size of H:V is 1:5) [m].

No of elements	130×130×75 [kPa]	150×150×75 [kPa]	200×200×100 [kPa]	250×250×150 [kPa]
≈ 2000	4762	2737	2510	2465
≈ 5000	9570	9870	9551	10109
≈ 16000	10686	10746	10695	10714
≈ 23000	10663	10631	10649	10599
≈ 32000	10635	10677	10594	10659
≈ 41000	10636	10622	10635	10575

The values in Tables 3.1 and 3.2 indicates that approximately 23000 elements and a geometry of 130×130×75 should be enough to calculate correct results. However, to make sure that the plastic deformations in the soil do not touch the boundaries of the model a domain of size 200×200×100 was used.

3.2.2 Cube model test

To test the precision of the numerical methods, simple scaled down cube models where tested to make sure that they are calculating correct results. These cubes where placed on and embedded in a soil with these parameters:

$\gamma = 1$ kN/m^3
$\phi = 37$ °
$c = 0$ kPa

in order to make easy comparisons to the theoretical value calculated with Equation 2.1. If the same inputs are used in Optum and LSG, the very same solution should appear or at least be close to it. To have a reliable comparison to LSG, which is also a numerical analysis method, it was made absolutely sure that the effects of nodal density and domain size are addressed, see Section 2.4.2.1.

3.2.2.1 Vertical loading

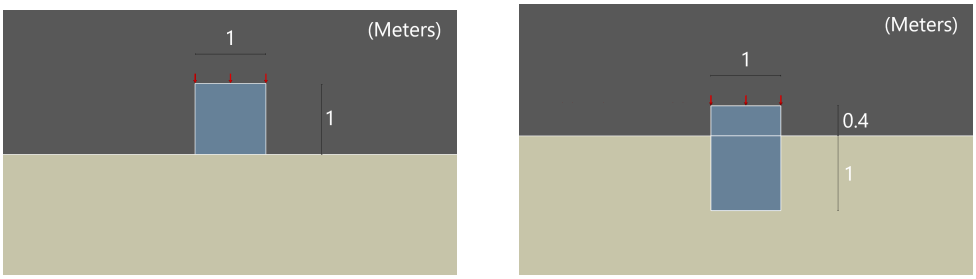

(a) 1×1, z=0 (b) 1×1.4, z=-1

Figure 3.4: Profile of cube model.

The first cube (Figure 3.4(a)) was a 1×1 meter large cube placed on the ground with evenly applied vertical loading on the top surface. According to the bearing capacity formula (Equation 2.1) the solution should be: $q = N_\gamma/2 = 24.2$ kN/m. The second cube (Figure 3.4(b)) was a 1×1.4 meter large cube embedded 1 meter underground, also with evenly applied vertical loading on the top surface. For this case the solution should be $q = N_\gamma/2 + N_q = 67.0$ kN/m. The result from the cube test can be seen in Table 3.3. The hand calculation and simulation in LSG, assume an infinitely long cube which is why the cube in Optum was tested for 100 meter long cube.

Table 3.3: Bearing capacity per meter for the cube test with evenly distributed vertical load on top surface.

Size, depth	Theoretical [kN/m]	LimitState:GEO [kN/m]	Optum 1 meter [kN/m]	Optum 100 meter [kN/m]
1×1, z=0	24.2	27	28.7	26.0
1×1.4, z=-1	67.0	99	263.8	113

For the 1×1 m large cube at depth z=0 the results are very similar for all methods. As for the 1×1.4 large cube at depth z=-1, the results are rather different between the methods. First of all, the difference between the 1 and 100 meter long cube in Optum is because of the surcharge from the soil having a larger impact when all sides of the cube are of equal length. This is why q is around twice as large for the 1 meter long cube than the 100 meter long. Secondly, the difference between the two numerical methods and theoretical hand calculation, which is about 30 percent lower, could be because of Equation 2.1 empirical nature which arguably is not the most effective method. Furthermore, it should be noted that LSG is upper bound while Optum is mixed solution which means that LSG in fact should be higher. However, the result between the two are close enough to arbitrate that the numerical methods works to a satisfactory level.

3.2.2.2 Moment of force loading

A test with moment of force loading was also made. For this test, the cube had to be given a weight of γ=10 kN/m^3. The moment was applied along a line in the middle of the top surface of the cube in Optum. For LSG, which is missing the feature to directly apply moment of force loading, two 0.1 meter long shearing forces was applied on the side surfaces of the cube, going in clockwise direction (Figure 3.5). Both forces was then multiplied with half the cube width as a lever, to get the resulting moment.

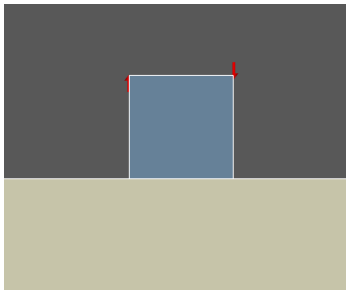

Figure 3.5: Applied shearing forces used in LimitState:GEO to calculate moment of force.

Table 3.4: Bearing capacity per meter for the cube test with moment of force loading applied to the upper part of the cube.

Size, depth	LimitState:GEO [kNm/m]	Optum 1 meter [kNm/m]	Optum 100 meter [kNm/m]
1×1, z=0	3.0	2.2	2.0
1×1.4, z=-1	7.8	8.9	7.6

The moment of force test showed very similar results between LSG and Optum. Especially the long cube in Optum because it is more similar to the case in LSG where the cube is infinitely long.

3.2.3 2D foundation model test

After it was concluded that the applied forces worked as intended a more detailed 2D model, similar to the real case model, was tested. A cross-section of the model can be seen in Figure 3.6 where most of the measurements are the same as the real foundation model with the exception of the top pedestal width and the bottom width. They are 5.8 and 21 meters instead of 6.6 and 23.8 meters. These measurements are based on the effective width of the real foundation. The soil's parameters are the same as for the real foundation model.

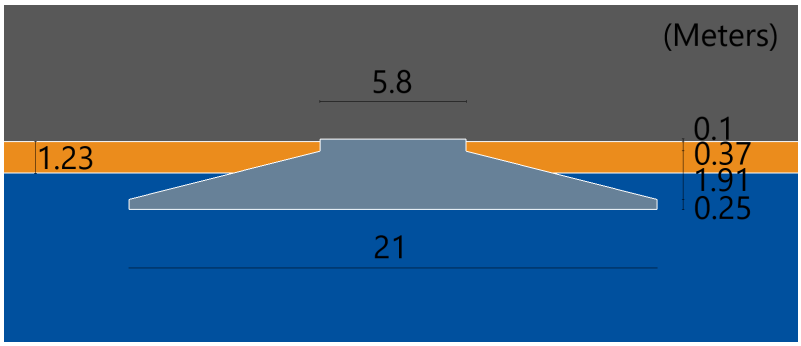

Figure 3.6: Cross section of 2D model

3.2.3.1 Vertical and horizontal loading

The 21×21 meter model should have similar results as the real case model, being a square with a side length based on the foundation model's effective width b_{eff} (Equation B.4). As for 21×420 meter model, it is 20 times longer than the width which means it should have similar results as LSG which is infinitely long.

Table 3.5: Stress level under foundation at ULS for vertical, horizontal and combined loading cases.

Load case	Theoretical	LimitState: GEO	2D Optum 21 meter	2D Optum 420 meter	Real case Optum
Vertical [kPa]	7931	10000	14948	10674	16571
Horizontal [kPa]	-	50	79	91	76
Vertical and horizontal ($V_{max}/2$, H_{max}) kPa	-	10553	16434	12048	17757

As with the cube test, the longer the 2D model is made the closer the results gets to LSG. When the 2D model is made 21×21 meters the result is moderately close to the real case model. The reason they are different is most likely because of the different shape of the bottom part.

3.2.3.2 Moment of force loading

A test with moment of force loading was made for this model as well. The moment was applied along a line in the middle of the top surface of the 2D model in Optum. For LSG, two 0.1 meter long shearing force was applied on the side surfaces above the soil going in clockwise direction. Furthermore, the real foundation's moment was multiplied with D1 and divided with D2 (see Figure 3.2), to make it comparable with the other results.

Table 3.6: Required moment of force loading at ULS.

Load case	LimitState:GEO	2D Optum 21 meter	2D Optum 420 meter	Real case Optum
Moment [kNm]	11867	16434	12048	17757

As expected, the real model and 21 meter long 2D model are similar in value while being higher than LSG and the 420 meter long 2D model. The latter two are also close in value as expected.

3.2.4 Remarks on verification of 3D model

The tests show that the foundation model that has been created in Optum calculates reasonable values. This has been shown for both vertical, horizontal and combined loading, as well as moment of force loading. Even though for some cases LSG gives lower values than the simulated 2D Optum, which in theory should not happen.

3.3 Creating yield surface for the shallow foundation

To create the yield surface, data of collapse loads is needed with different configurations of applied vertical, horizontal and moment of force loading. When the data is collected, first only the vertical force V_{max} is calculated. Thereafter, the acting vertical force is fixed at different intervals between 0 and V_{max} with different combination of horizontal and moment loading. The series of fixed vertical loading and all the load combinations of M and H that was used are found in tables A.1 and A.2 in the appendix.

With sufficient data the yield surface starts to take shape. The data, which at this stage is in the form of a 3D point cloud, is then triangulated by Delaunay triangulation to create surfaces between the points in matlab. The surfaces is then smoothed out by using the matlab-based mesh generation and processing toolbox iso2mesh developed by Fang (2017).

After the yield surface mesh has been created, a yield surface equation was constructed. This equation was based on Butterfield and Gottardi (1994) proposed formula in 2.5.

The created yield surface gives a visual representation of the failure loads. For comparison, the method of using the drained bearing capacity formula (Equation 2.1), is shown in Appendix C.

3.3.1 Design load cases

The following design load cases were provided from the wind turbine manufacturer. They are load cases that should be considered and checked for, to not produce failure

of the soil.

Table 3.7: Design load combinations for wind turbine foundation.

Design load case	Vertical [kN]	Moment [kNm]	Horizontal [kN]
Lift-off	5517	72386	569
Overturning	5552	122168	994
Sliding	5469	49162	442
Shear failure	7208	134413	1083

4
Results

4.1 Yield surface

Figure 4.1 shows the calculated point values from Optum and the generated mesh. It can be noted that the points calculated above $V \approx 6{\times}10^6$ are less smooth than the rest of the points.

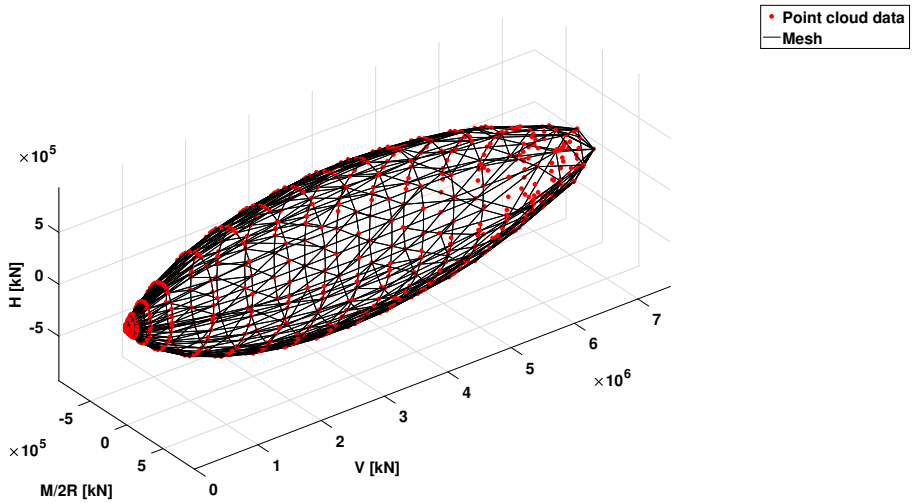

Figure 4.1: Overview of collected point cloud data and generated mesh.

The yield surface presents a more accurate picture of where the ULS lies than just using the drained bearing capacity formula. As can be seen in Appendix C, using Equation 2.1 results in a single stress value at shear failure. To check for other risks, such as sliding or overturning, further calculation needs to be made. In a very visual way, the yield surface illustrates how each of the three loading types impacts the overall stability of the construction. For example, if the vertical load is decreased it will reduce the overall stability if horizontal and moment loading stays the same.

The created yield surface, or failure envelope, have been compared with Butterfield and Gottardi's values of the horizontal and moment loading that would cause failure, i.e. $H_{max} \approx V_{max}/8$ and $M_{max}/2R \approx V_{max}/11$ at $V_{max}/2$. The result in Table 4.1 shows V_{max}, $M_{max}/2R$ and H_{max} (first column). $M_{max}/2R$ and H_{max} are situated in the middle of the yield surface at $V_{max}/2$. The values are normalized by dividing the

results with V_{max} (second column). These values are then compared to Butterfield and Gottardis values (third column) by calculating the ratio of the two values (fourth column). The ratio is close to 1 for both H_{max} and $M_{max}/2R$ which proves that the created failure envelope has a similar shape as the one suggested by Butterfield and Gottardi (1994).

Table 4.1: V_{max}, H_{max} and $M_{max}/2R$, and a normalization of said values to be compared with Butterfield and Gottardi (1994).

		Butterfield and Gottardi		
	Result [kN]	$\frac{1}{V_{max}}$ %	$\frac{1}{V_{max}}$ %	Ratio
V_{max}	7375890	100	100	1
M_{max}/2R	598076	8.1	9.1	0.89
H_{max}	904564	12.3	12.5	0.98

4.1.1 Yield surface equation

With Equation 2.5 as its archetype, Equation 4.1 is a normalized formula that correlates with the calculated point cloud data from the case study.

$$\frac{(2.149\frac{H}{V_{max}})^2 - 5.331\frac{H}{V_{max}}\frac{M}{2RV_{max}} + (3.312\frac{M}{2RV_{max}})^2}{(\frac{V+5DW}{V_{max}}(1-\frac{V+5DW}{V_{max}}))^2} = 1 \tag{4.1}$$

DW = deadweight force of the foundation [kN]

By calculating the slope angles t_h, t_m and ρ and adding a parameter DW multiplied with 5, to account for the soil's inertia effects on the bearing capacity, it was possible to find an equation that calculates similar result as the yield surface mesh. Figures 4.2-4.5 shows multiple cross-sections to illustrate this similarity. However, Figure 4.3 shows that the mesh has relatively small to no inclination in the $M/2R$-H plane at small V, unlike the equation.

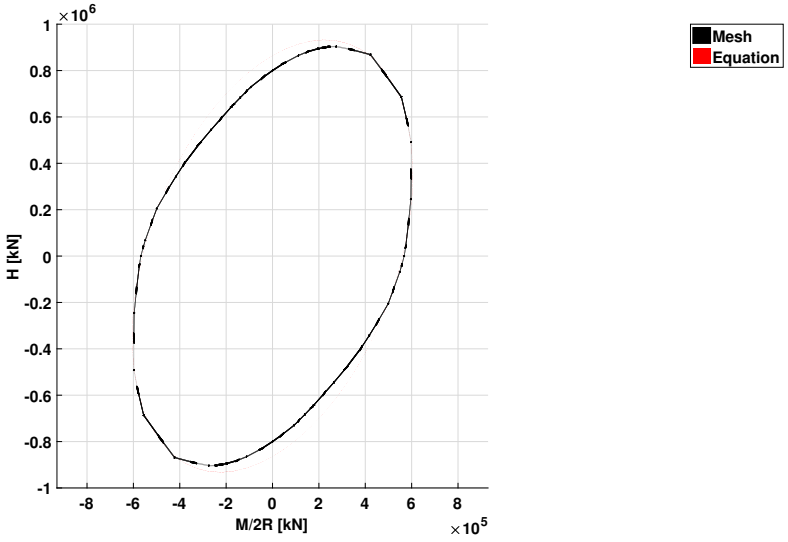

Figure 4.2: Yield surface mesh and equation from moment/2R-horizontal view at V=Vmax/2.

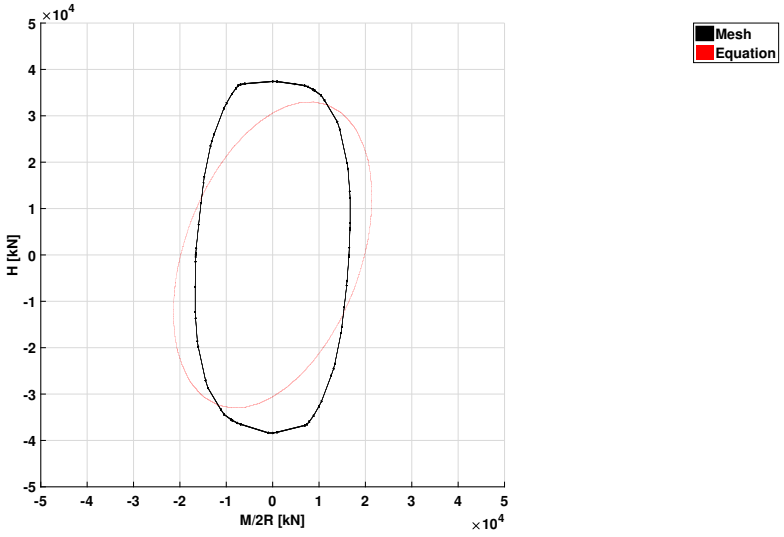

Figure 4.3: Yield surface mesh and equation from moment/2R-horizontal view at V=5000 kN.

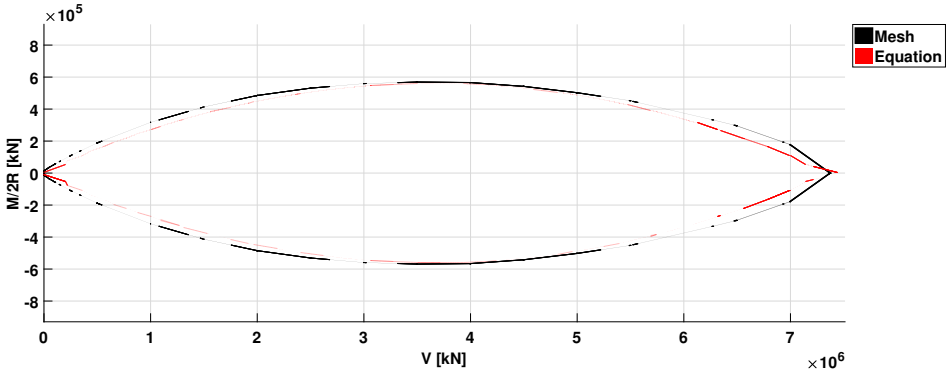

Figure 4.4: Yield surface mesh and equation from vertical-moment/2R view at H=0.

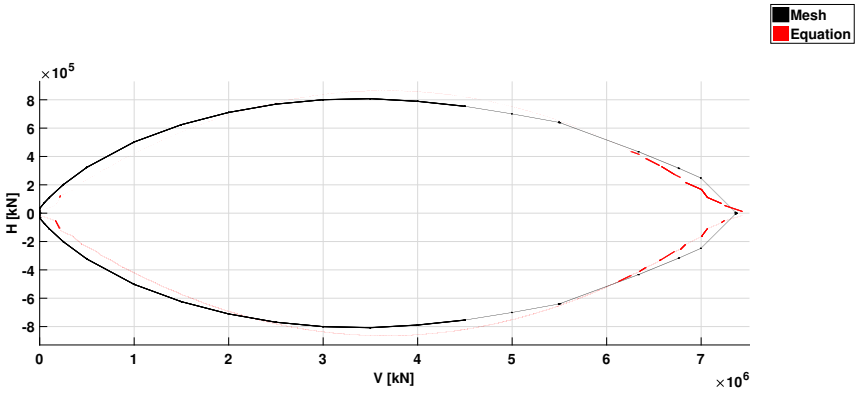

Figure 4.5: Yield surface mesh and equation from vertical-horizontal view at moment/2R=0.

A close-up of Figure 4.4 and 4.5 at V=0 kN to V=1×10^6 kN can be seen in Appendix D.

4.2 V_{max}, H_{max} and $M_{max}/2R$ for differently scaled foundation

To test if the yield surface equation (Equation 4.1) is valid for the same foundation, but scaled differently, further simulations in Optum were made with reduced foundation sizes. Table 4.2 showcases V_{max}, $M_{max}/2R$ and H_{max} (first, second and third

column) for differently scaled foundations. It also shows the normalization of H_{max} and $M_{max}/2R$ by dividing said value with their corresponding V_{max} (fourth and fifth column). The first row is the normally scaled foundation, that is to say it has the measurements shown in Figure 3.2. The foundations on the second and third row have the same relative measurements as the first, but the size has been reduced by 25 % and 50 %.

Table 4.2: V_{max}, H_{max} and $M_{max}/2R$, as well as normalized H_{max} and $M_{max}/2R$ in regards to V_{max}, for foundations of the different scales 1, 3/4 and 1/2.

Scale	V_{max} [kN]	$M_{max}/2R$ [kN]	H_{max} [kN]	$M_{max}/2RV_{max}$ %	H_{max}/V_{max} %
1	7375890	598076	904564	8.1	12.3
3/4	3160921	262974	391889	8.3	12.4
1/2	999382	82694	122855	8.3	12.3

Since the scaled down yield surfaces show similar result between each other, it is reasonable to believe that Equation 4.1 is valid for all of them. It is true for this particular footing shape in this particular soil and if the equation is known it is easy to substitute the values of V_{max} and DW. However, if the shape of the footing or the soil parameters are tweaked, it is unknown how this would affect the equation. It is possible that a whole new yield surface would have to be created. Making a yield surface in the manner presented in this study is time consuming and may be unnecessary thorough.

4.2.1 Cross-sections of yield surface for design load cases

Figures 4.6(a), 4.6(b), 4.6(c) and 4.6(d) shows a cross-section of the yield surface, created with Equation 4.1, with differently scaled foundations at the particular vertical loading specified for each design load case shown in Table 3.7.

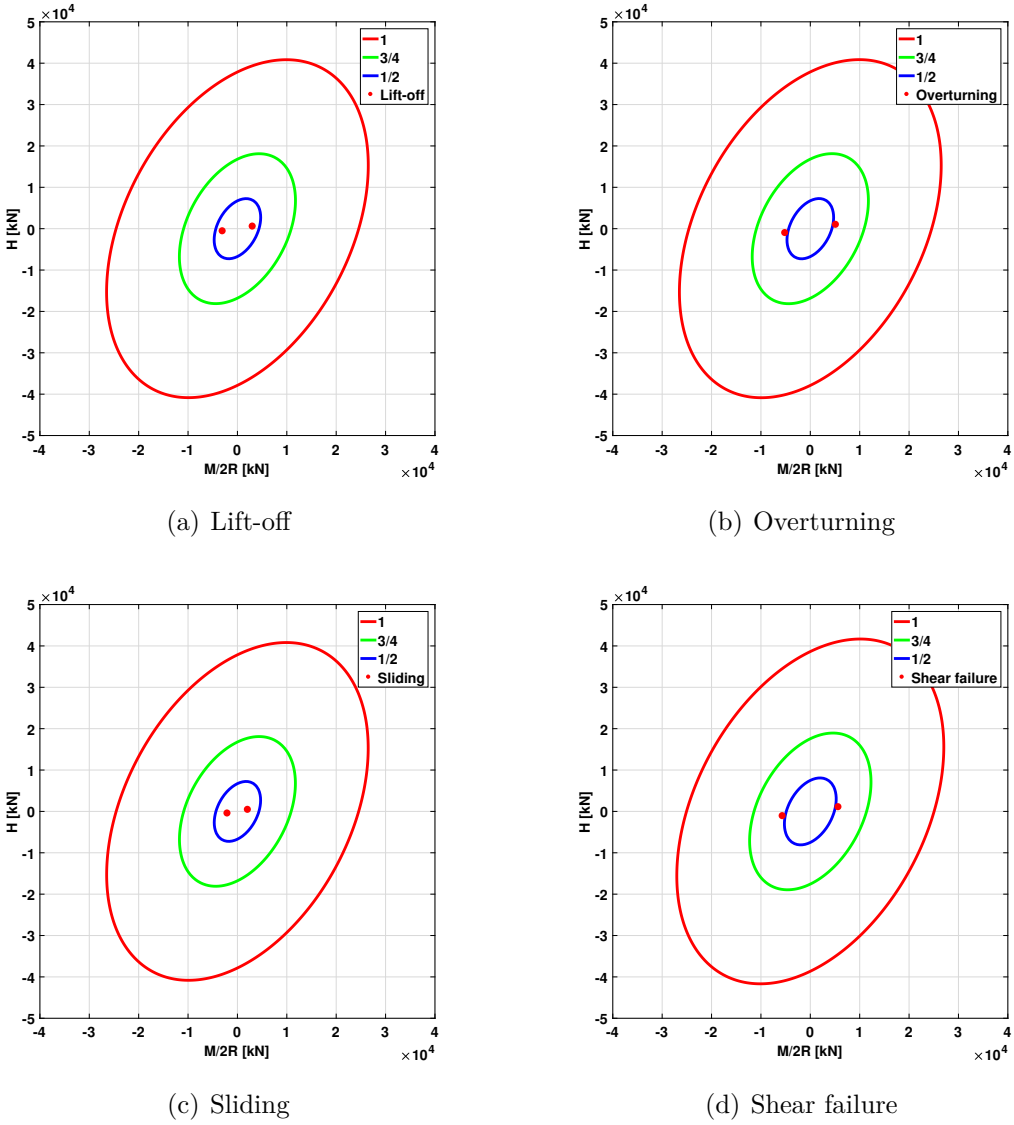

(a) Lift-off

(b) Overturning

(c) Sliding

(d) Shear failure

Figure 4.6: Cross sections of the yield surface for the load cases.

The cross-section's of the yield surface with the corresponding design load cases, show that the foundation is quite overdimensioned for the normally sized foundation. The yield surface is 5-fold greater than the overturning design case (Figure 4.6(b)), which is the one that has the biggest risk. At 1/2 the original size, all of the design cases are situated close to the failure envelope. It can be seen that if the foundation size is reduced, the failure surface decreases with an increasing rate. With a smaller foundation, material usage can be reduced. A consequence of smaller foundation size is that the contact pressure will be larger, hence settlements will increase under static loads. As a result the density of the soil will increase. As Wichtmann (2005) showed for sand and possibly for this coarse grained till as well, the dynamic properties, G_{max} and damping will change: G_{max} will mainly increase due to increased effective stress level while the damping increases due to the larger density of the soil.

4.3 Remarks

For the purpose of this study, it would have been convenient to retrieve the resulting strains from the model in Optum under working loads. Unfortunately, this was not possible in the current version of the program as at the time of writing this report post processing is rather sparse.

The foundation material was assumed rigid. This certainly would have an impact on the results, however, possibly quite small. Would the foundation material have been flexible, the failure load would potentially have been greater. With an elastic foundation it would be a more uniform contact pressure distribution but the settlements would increase (Leshchinsky and F. Marcozzi, 1990).

Using a 3D numerical analysis tool such as Optum, means that the calculated results will reflect more accurately the reality. It accounts for eccentric and non uniformed loading distribution that the structure is subjected to, instead of using approximating factors such as in the bearing capacity formula.

5
Conclusions & Recommendations

5.1 Conclusions

A shallow foundation has been analyzed with three different methods and results has been compared with each other, bearing capacity formula, LimitState:GEO and Optum G3. The results are in good agreement with each other and it has been shown that Optum G3 is an efficient tool to analyze more complex problems, such as combined loading in coarse grained material.

A yield surface equation has been created that is valid for the prerequisites, soil parameters and shape of foundation of this study. The same yield surface equation is valid for different sizes of the foundation. Resulting yield surface satisfies previously published yield surface theory by Butterfield and Gottardi (1994).

From a stability point of view, it has been demonstrated that the foundation in this study is oversized and could be designed to be smaller. The foundation has not been checked for other requirements, however, like settlements and dynamic stiffness. It is not uncommon that these latter requirements control the design of the foundation.

5.2 Recommendations

For further investigations, the following topics are recommended:

- Settlements under working loads.
- The influence of different foundation geometries on yield surface (e.g. square foundation).
- Sensitivity analysis of soil parameters and water influence on yield surface.
- Investigation of dynamic stiffness as a function of frequency, amplitude and numbers of cycles for different soil types.
- Elastic foundations influence on dynamic response.

Bibliography

Ahmed, A. and Soubra, A.-H. (2014). Reliability analyses at ultimate and serviceability limit states of obliquely loaded circular foundations. *Geotechnical and Geological Engineering*, 32(4):729–738.

Asp, M. (2016). Vad väger betong – beroende på hur många kubikmeter. [Online; accessed 2018-05-08].

Bhattacharya, S. (2017). The e&t energy and power hub.

Boverket (2009). *Vindkraftshandboken: Planering och prövning av vindkraftverk på land och i kustnära vattenområden*. Boverket.

Burton, T., Jenkins, N., Sharpe, D., and Bossanyi, E. (2011). *Wind energy handbook*. John Wiley & Sons.

Butterfield, R. and Gottardi, G. (1994). A complete three-dimensional failure envelope for shallow footings on sand. *Géotechnique*, 44(1):181–184.

Byrne, B. (2011). Foundation design for offshore wind turbines. [Online; accessed 2018-05-17].

Byrne, B. W. (2000). *Investigations of suction caissons in dense sand*. PhD thesis, University of Oxford Oxford, UK.

DNV (2002). *Guidelines for design of wind turbines*. Det Norske Veritas.

Energimyndigheten (2014). Vindkraftsforsning. [Online; accessed 2018-03-05].

Fang, Q. (2017). iso2mesh. [Online; accessed 2018-05-02].

Froese, M. (2017). Ge delivers largest onshore wind farm in europe. [Online; accessed 2018-03-05].

Gilbert, M., Smith, C., Haslam, I., and Pritchard, T. (2010). Application of discontinuity layout optimization to geotechnical limit analysis problems. In *Proceedings of the 7th European Conference in Numerical Methods in Geotechnical Engineering, Trondheim*, pages 169–174.

IEG (2010). Rapport 7:2008, tillämpningsdokument, en 1997-1 kapitel 6 plattgrundläggning.

Jacobsson, S., Karltorp, K., and Dolff, F. (2014). Towards a strategy for offshore wind power in sweden.

K Krabbenhoft, AV Lymain, J. K. (2016a). Optumg2: Materials. [Online; accessed 2018-04-29].

K Krabbenhoft, AV Lymain, J. K. (2016b). Optumg2: Theory. [Online; accessed 2018-04-29].

Knappett, J. (2012). *Craig's soil mechanics*, volume 8. Spon Press London, UK.

Leshchinsky, D. and F. Marcozzi, G. (1990). Bearing capacity of shallow foundations: Rigid versus flexible models. 116.

LimitState (2016). *LimitState:GEO Manual*. Ltd. The Innovation Centre 217 Portobello Sheffield S1 4DP United Kingdom, 3.4.a edition.

Mohamed, W. M. M. (2016). Windmill foundations on weak soils.

Ntambakwa, E., Yu, H., Guzman, C., and Rogers, M. (2016). Geotechnical design considerations for onshore wind turbine shallow foundations.

Prandtl, L. (1920). Über die härte plastischer körper. *Nachrichten von der Gesellschaft der Wissenschaften zu Göttingen, Mathematisch-Physikalische Klasse*, 1920:74–85.

Senetakis, K., Anastasiadis, A., and Pitilakis, K. (2013). Normalized shear modulus reduction and damping ratio curves of quartz sand and rhyolitic crushed rock. *Soils and Foundations*, 53(6):879–893.

SGI (2018). Jordarter. [Online; accessed 2018-03-05].

Shrestha, S. and Ravichandran, N. (2015). Design and analysis of foundations for onshore tall wind turbines. In *Geo-Chicago 2016*, pages 217–226.

Sloan, S. (2013). Geotechnical stability analysis. *Géotechnique*, 63(7):531.

Terzaghi, K. (1944). *Theoretical soil mechanics*. Chapman And Hali, Limited John Wiler And Sons, Inc; New York.

Verruijt, A. and Van Baars, S. (2007). *Soil mechanics*. VSSD Delft, the Netherlands.

Warren-Codrington, C. J. (2013). *Geotechnical considerations for onshore wind turbines: adapting knowledge and experience for founding on South African pedocretes*. PhD thesis, University of Cape Town.

Wichtmann, T. (2005). *Explicit accumulation model for non-cohesive soils under cyclic loading*. PhD thesis, Inst. für Grundbau und Bodenmechanik Bochum University, Germany.

A

Appendix

Table A.1: Total fixed vertical load applied on the pedestal that was used when calculating the combined loading of M and H.

Vertical [kN]
0
50000
100000
250000
500000
1000000
1500000
2000000
2500000
3000000
3500000
4000000
4500000
5000000
5500000
6000000
6500000
7000000

Table A.2: The load combinations used in the data collection simulations for each series of fixed vertical load.

Moment [kNm/m]	Horizontal load [kN/m^2]
300	0.01
-300	0.01
300	0.3
-300	0.3
300	1
-300	1
300	2
-300	2
300	3
-300	3
300	5
-300	5
300	8
-300	8
300	10
-300	10
300	12
-300	12
300	18.8
-300	18.8
0	8
300	0

B

Appendix

The calculations for bearing capacity are usually made with design parameters, e.g Eurocode. The material factors γ_c and γ_ϕ are chosen depending the safety class and whether it is a drained or an undrained analysis. The design values of the soil's strength parameters can be calculated as follows:

$$c_d = \frac{c}{\gamma_c} \quad \text{and} \quad \phi_d = \frac{arctan(\phi)}{\gamma_\phi} \tag{B.1}$$

Shape factors s are calculated as follows:

$$s_\gamma = 1 - 0.4\frac{b_{eff}}{l_{eff}} \quad s_q = s_c = 1 + 0.2\frac{b_{eff}}{l_{eff}} \tag{B.2}$$

and inclination factors i as follows:

$$i_q = i_c = (1 - \frac{H_d}{V_d + A_{eff}c_d cot\phi_d})^2 \quad i_\gamma = i_q^2 \tag{B.3}$$

The effective foundation area of a circular foundation can be represented as a rectangle (see Figure B.1) with the following dimensions:

$$l_{eff} = \sqrt{A_{eff}\frac{l_e}{b_e}} \quad \text{and} \quad b_{eff} = \frac{l_{eff}}{l_e}b_e \tag{B.4}$$

where

$$A_{eff} = 2[R^2 arccos(\frac{e}{R}) - e\sqrt{R^2 - e^2}] \tag{B.5}$$

$$e = \frac{M_d}{V_d} \tag{B.6}$$

$$b_e = 2(R - e) \tag{B.7}$$

$$l_e = 2R\sqrt{1 - (1 - \frac{b_e}{2R})^2} \tag{B.8}$$

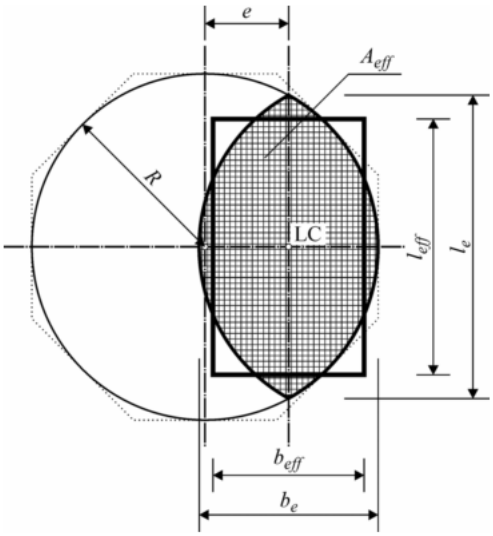

Figure B.1: Real area and effective area of circular foundation

C
Appendix

Hand calculation for design case shear failure.

Design case "Shear failure"									
Md	134413,2	kNm		d1	1,23	m			
V	7207,9	kN		d2	1,45	m			
phi	37	degrees		gamma	20	kN/m3			
c	0	kPa		gamma'	12	kN/m3			
Hd	1082,5								
V_f	614,2	m3							
uw_f	25	kN/m3							
DW	20729,3	kN	V_f*uw_f*1,35						
Vd	27937,2		V+DW						
e	4,8	m	Md/Vd						
R	11,9	m							
A_eff	222,3	m2							
b_e	14,2	m							
l_e	21,8	m							
l_eff	18,5	m							
b_eff	12,0	m							
In accordance with EC7:									
PF_frictionA	1,25	-							
PF_gamma	1	-							
PF_c	1,25	-	partial factors						
phi_d	31,1	degrees							
N_gamma	17,5	-	s_gamma	0,74	-	i_gamma	1,08	-	
N_c	32,9	-	s_c	1,13	-	i_c	1,04	-	
N_q	20,8	-	s_q	1,13	-	i_q	1,04	-	
gamma_exv	13,0	kN/m3							
p0'	42	kPa							
q_d	2116,0	kN/m2							

D

Appendix

Yield surface mesh and equation from vertical-moment/2R and from vertical-horizontal view at V=0 to V=1000000.